

Local Group Ultra-Faint Dwarf Galaxies in the Reionization Era

Daniel R. Weisz¹, Michael Boylan-Kolchin²

¹*Department of Astronomy, University of California Berkeley, Berkeley, CA 94720, USA; dan.weisz@berkeley.edu*

²*Department of Astronomy, The University of Texas at Austin, 2515 Speedway, Stop C1400, Austin, TX 78712-1205, USA*

22 February 2017

ABSTRACT

Motivated by the stellar fossil record of Local Group (LG) dwarf galaxies, we show that the star-forming ancestors of the faintest ultra-faint dwarf galaxies (UFDs; $M_V \sim -2$ or $M_\star \sim 10^2$ at $z = 0$) had ultra-violet (UV) luminosities of $M_{UV} \sim -3$ to -6 during reionization ($z \sim 6 - 10$). The existence of such faint galaxies has substantial implications for early epochs of galaxy formation and reionization. If the faint-end slopes of the UV luminosity functions (UVLFs) during reionization are steep ($\alpha \lesssim -2$) to $M_{UV} \sim -3$, then: (i) the ancestors of UFDs produced $> 50\%$ of UV flux from galaxies; (ii) galaxies can maintain reionization with escape fractions that are > 2 times lower than currently-adopted values; (iii) direct HST and JWST observations may detect only $\sim 10 - 50\%$ of the UV light from galaxies; (iv) the cosmic star formation history increases by $\gtrsim 4 - 6$ at $z \gtrsim 6$. Significant flux from UFDs, and resultant tensions with LG dwarf galaxy counts, are reduced if the high-redshift UVLF turns over. Independent of the UVLF shape, the existence of a large population of UFDs requires a non-zero luminosity function to $M_{UV} \sim -3$ during reionization.

Key words: dark ages, reionization, first stars – early universe – stellar content – Local Group

1 INTRODUCTION

Low-mass galaxies appear to play a central role in ionizing the neutral intergalactic medium (IGM) in the early Universe. While sources such as AGN and X-ray binaries may contribute ionizing photons (e.g., McQuinn 2012; Madau & Haardt 2015), the consensus view is that a large population of low-mass galaxies is required to explain the observed ionization fraction of the IGM and the Thomson optical depth (τ_e) during reionization (e.g., Stark 2016).

However, the low-mass galaxy population associated with reionization has never been directly detected. The deepest available blank-field *Hubble Space Telescope* (HST) observations only reach $M_{UV}(z \sim 7) \sim -16$ (e.g., Finkelstein et al. 2015; Bouwens et al. 2015), but contemporary models of the high- z Universe (e.g., Kuhlen et al. 2012; Robertson et al. 2013, 2015) require the ultra-violet luminosity function (UVLF) to remain steep to magnitudes as faint as $M_{UV}(z \sim 7) = -10$ in order for galaxies to maintain reionization. Gravitational lensing and the exquisite sensitivity of the *James Webb Space Telescope* (JWST) promise to push observations further down the galaxy UVLF (e.g., to $M_{UV}(z \sim 7) \sim -14$), but the direct detection and characterization of a significant number of intrinsically faint galax-

ies ($M_{UV} \sim -10$) in the reionization era appears beyond observational capabilities for the foreseeable future. Consequently, the contribution of low-mass galaxies to reionization will continue to be estimated by extrapolating the observed UVLF to galaxies that cannot be directly observed.

Concurrent with searches for faint galaxies at high redshifts, there has been a renaissance in the discovery of extremely faint, low-mass galaxies in the Local Group (LG; e.g., Willman et al. 2005; Belokurov et al. 2006, 2010; Irwin et al. 2007; Koposov et al. 2007; Zucker et al. 2006a,b; Kim et al. 2015; Koposov et al. 2015; Laevens et al. 2015a,b; Martin et al. 2015; Bechtol et al. 2015). Deep, wide-field photometric surveys (e.g., SDSS, DES) have identified dozens of faint galaxies surrounding the Milky Way (MW) with luminosities as low as $M_V \sim -2$ ($M_\star \sim 10^2 M_\odot$), and these detections likely represent only a fraction of the low-mass galaxy population in the Local Group owing to various observational biases (e.g., Koposov et al. 2008; Tollerud et al. 2008; Walsh et al. 2009). These so-called ‘ultra-faint’ dwarf galaxies (UFDs) host predominantly ancient (> 13 Gyr), extremely metal-poor ($[Fe/H] < -2$) stellar populations (e.g., Frebel & Norris 2015). They are therefore consistent with being ‘fossils of reionization’ (e.g., Ricotti & Gnedin 2005; Okamoto et al. 2012; Brown et al.

2014; Weisz et al. 2014b): UFDs were star-forming galaxies in the early Universe until UV radiation associated with cosmic reionization stunted their formation (e.g., Bovill & Ricotti 2009).

Though the connection between reionization and truncated star formation in UFDs appears well-established, the possible contribution of the ancestors of UFDs – low-mass star-forming galaxies – to cosmic reionization is far less appreciated.¹ In this letter, we address this point by combining the observed stellar fossil record of UFDs around the MW with stellar population synthesis models in order to quantify the role of UFDs in reionizing the early Universe. Specifically, we infer the evolution of the UV luminosities of the lowest-mass UFDs across cosmic time and explicitly estimate (i) M_{\min} , the minimum UV luminosity of star-forming galaxies during the epoch of reionization and (ii) the effects such systems have on our understanding of the high-redshift ($z \gtrsim 6$) Universe. Throughout this paper, we adopt a Planck Collaboration et al. (2016) cosmology.

2 METHODOLOGY

We combine the star formation histories (SFHs) of UFDs located around the MW measured from the stellar fossil record with the Flexible Stellar Population Synthesis code (FSPS; Conroy et al. 2009, 2010) to compute their integrated UV luminosities as a function of redshift. This methodology is detailed in Weisz et al. (2014c) and Boylan-Kolchin et al. (2015). Here, we summarize the technique and briefly describe assumptions specific to this analysis.

The SFHs of UFDs have been measured by analyzing deep *HST*-based color-magnitude diagrams (CMDs) for a dozen galaxies located in the immediate vicinity of the MW (e.g., Brown et al. 2014; Weisz et al. 2014a). From measurements, we construct a fiducial SFH of an UFD: 70% of its total stellar mass ($M_{\star}(z=0) \sim 5 \times 10^2 M_{\odot}$) forms in a ~ 100 Myr interval between $z \sim 9-11$, and the remaining 30% forms over a ~ 2.5 Gyr period that ends at $z \sim 3$. This SFH is consistent with observations of Local Group UFDs (e.g., Brown et al. 2014; Weisz et al. 2014b) and fits well with a scenario in which the UV background suppresses the accretion of fresh gas onto UFDs, as opposed to photo-evaporating existing cold gas, allowing for (very) low-level star formation to continue post-reionization (e.g., Oñorbe et al. 2015).

This baseline SFH is plotted in the top panel of Figure 1, and the bottom panel of the figure shows the corresponding integrated UV (black) and V-band (orange) flux evolution. We construct these profiles using FSPS, a Kroupa IMF (Kroupa 2001), the Padova stellar evolution models (Girardi et al. 2010), and a single metallicity of $[\text{Fe}/\text{H}] = -2.0$. We assume no dust, which is consistent with the observed spectral energy distributions (SEDs) of the faintest high-redshift galaxies (e.g., Bouwens et al. 2014). Finally, we normalize the computed fluxes to have $M_V(z=0) = -2$, a value comparable to the faintest known UFDs around the MW (cf. McConnachie 2012).

Our fiducial model is designed to broadly reflect the

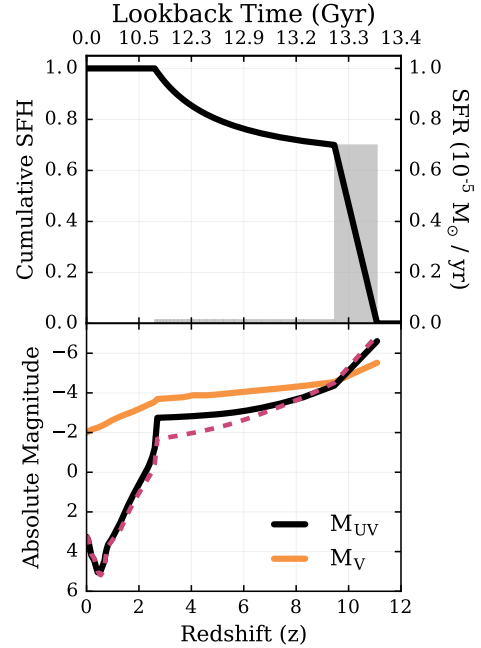


Figure 1. *Top* – The SFH of our fiducial UFD, which is motivated by the stellar fossil record of UFDs found orbiting the MW. The grey shading indicates the absolute SFR as a function of time and the solid black line represents the normalized cumulative SFH. Patterned after analysis of deep *HST*-based CMDs of UFDs located around the MW, our fiducial UFD formed 70% of between $z \sim 9-11$ and 30% of its stellar mass from $z \sim 3-9$. The total stellar mass of this system is $\sim 5 \times 10^2 M_{\odot}$, which is comparable to the faintest known galaxies in the Local Group. *Bottom* – The evolution of M_V (orange) and M_{UV} (black) vs. redshift for our fiducial UFD. The present day luminosity, $M_V = -2$, is comparable to the faintest known UFDs. The magenta dashed line indicates the evolution of M_{UV} if UFD formed 90% of its stellar mass in the initial event instead of 70%.

behavior of a typical UFD, not encompass all possible scenarios. To illustrate the effects of another plausible SFH, we consider the case in which 90% of the stellar mass formed from $z \sim 9-11$. The difference in the UV flux between this alternate SFH and our default model is no more than 0.5 mag (magenta-dashed line in Figure 1). Beyond varying the SFH, other physical effects (e.g., interacting binaries, stochastic sampling of the IMF, or various burst permutations of the SFHs; Fumagalli et al. 2011; Weisz et al. 2012; Domínguez et al. 2015; Stanway et al. 2016) can affect the UV and ionizing flux output from a galaxy. However, the amplitude of these effects (typically 1-2 mag) are not sufficiently large to change the main conclusions of this paper.

3 RESULTS AND DISCUSSION

Figure 1 illustrates the main result of this paper: *the stellar fossil record in the Local Group demonstrates that star-forming galaxies as faint as $M_{UV} = -3$ existed during the epoch of reionization ($z \sim 6-10$).* Over that period, the UV magnitudes of such objects initial declines by ~ 3 mag, as expected from a constant SFH from $z \sim 9-11$. This period is followed by a gradual decline in integrated UV and opti-

¹ Especially by Brian.

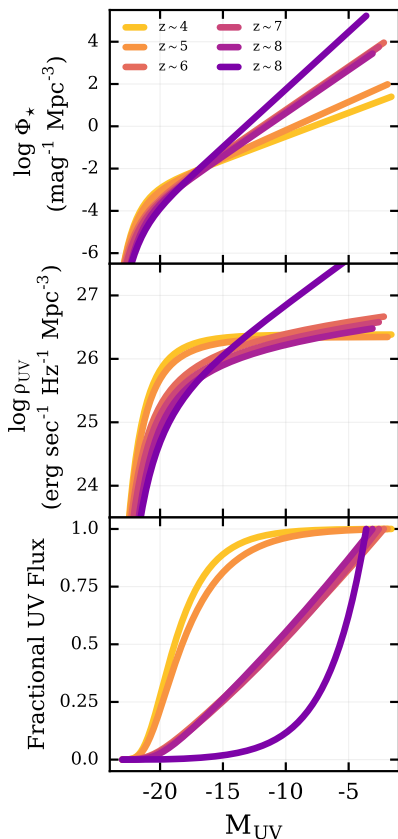


Figure 2. *Top* – Schechter UVLFs from $z \sim 4 - 8$ from Finkelstein et al. (2015), along with a $z \sim 8$ UVLF from Bouwens et al. (2015), based on direct measurements of distant galaxies. The UVLFs are plotted to $M_{UV} \sim -3$, the approximate faint magnitude limit based on the stellar fossil record of UFDs found in the LG. Values of the faint-end slopes range from $\alpha \sim -1.6$ at $z \sim 4$ to $\alpha \sim -2.4$ at $z \sim 8$. *Middle* – The integrated UV flux for the UVLFs in the top panel, plotted as a function of UV magnitude. *Bottom* – The fraction of UV flux as a function of M_{UV} for the Schechter UVLFs plotted in the top panel, integrated to values plotted in Figure 1. For $z \gtrsim 6$, UFDs contribute 50-90% of the total UV flux from galaxies.

cal flux from $z \sim 3 - 9$, when the SFH is constant but lower by a factor of ~ 10 relative to its peak. Once star formation shuts off at $z \sim 3$, the UV flux falls off precipitously owing to the rapid death of UV-luminous young stars. Over the same period, the optical luminosity declines more gradually, as it originates from stars with a wider range of masses. Finally, the upturn in UV luminosity at late times ($z \lesssim 0.2$) stems from the onset of blue horizontal branch stars, which dominate the UV light in the absence of young stars.

3.1 Assuming Steep Luminosity Functions and Faint Star-Forming Galaxies

The number density of star-forming galaxies in the early Universe appears well-described by a Schechter function with a faint-end slope that steepens with increasing redshift (e.g., Bouwens et al. 2015; Finkelstein et al. 2015). In this section, we briefly explore the consequences of assuming this functional form of the UVLF remains valid into the regime of

UFDs. We consider the alternative – that the high- z UVLF breaks to a shallower slope – in Section 3.2.

3.1.1 Reionization

Scenarios for galaxy-driven reionization typically require integration of the UVLF to a lower luminosity limit of $M_{\min} = -10$ to -13 at $z \gtrsim 6$ (e.g., Kuhlen et al. 2012; Robertson et al. 2013, 2015). However, the faint ancestors of UFDs extend M_{\min} fainter by an additional ~ 7 magnitudes. The $M_{UV}(z)$ values for our fiducial UFD more accurately reflect the true lower luminosity limit of star-forming galaxies in the early Universe.

Figure 2 shows that extending M_{\min} into the regime of UFDs (again, assuming the faint-end slope of the LF remains unchanged) results in a substantial increase in the amount of total UV (and, by extension, ionizing) flux produced by faint galaxies. The smallest flux contribution from UFDs is at low redshifts ($z \sim 4 - 5$), where the faint-end slope is fairly flat ($\alpha \sim -1.5$ to -1.7); over 90% of the flux is generated by galaxies brighter than $M_{UV} = -10$. Faint galaxies make a larger contribution at $z \sim 6 - 7$, as the faint-end slope is steeper ($\alpha \sim -2$). Galaxies fainter than current *HST* blank-field limits ($M_{UV} \sim -16$) contribute 80% of the total UV flux. Thus, the deepest direct observations of the early Universe only resolve 20% of the total UV light from galaxies. Further, galaxies fainter than $M_{UV} = -10$, contribute $\sim 50\%$ of the total UV flux. Future blank-field observations with *JWST* are projected to extend to $M_{UV} \sim -14$, which will resolve $\sim 40\%$ of the total UV flux from galaxies.

Some observation suggest that the faint-end slope may be as steep as ~ -2.4 at $z \sim 8$ (e.g., Finkelstein et al. 2015), increasing the importance of faint galaxies. Although uncertainties remain large (~ 0.4 dex), we consider two UVLFs at $z \sim 8$, with $\alpha = -2.02$ and -2.36 (Bouwens et al. 2015; Finkelstein et al. 2015). For the shallower slope, the contribution of faint galaxies is identical to the $z \sim 6 - 7$ scenario. For the steeper slope, $>85\%$ of the instantaneous UV flux comes from galaxies fainter than $M_{UV} = -10$. In either case, the deepest blank-field *HST* and future *JWST* observations are only sensitive to at most $\sim 10\%$ of the UV light. This trend may continue at even higher redshifts ($z \sim 9 - 10$), as current measurements appear to favor faint-end slopes of $\alpha \sim -2.3$ (e.g., Bouwens et al. 2016), albeit with large uncertainties.

Additional UV and ionizing flux from UFDs implies that galaxies could maintain reionization with smaller escape fractions (f_{escape}) for ionizing photons. For example, Robertson et al. (2013) assume $f_{\text{escape}} = 0.2$, $\alpha \sim -2$, $M_{\min} \sim -10$ for galaxies to maintain reionization. However, adopting $f_{\text{escape}} = 0.1$ and $M_{\min} = -3.1$ yields the same total ionizing flux. If the faint-end slope is as steep as $\alpha \sim -2.4$, then $f_{\text{escape}} = 0.02$ and $M_{\min} = -3.1$ would also maintain reionization. Values of f_{escape} between ~ 2 and 10% appear consistent with several observational and theoretical results (e.g., Leitert et al. 2013; Siana et al. 2015; Ma et al. 2015).

Extra UV flux from UFDs could also imply a higher ionization fraction of the IGM at times earlier than indicated by Planck Collaboration et al. (2016). That is, if UFDs formed early enough and the UVLF was sufficiently steep, then UFDs may have provided enough flux to initiate reionization earlier than $z \sim 10$. While an interesting potential conflict,

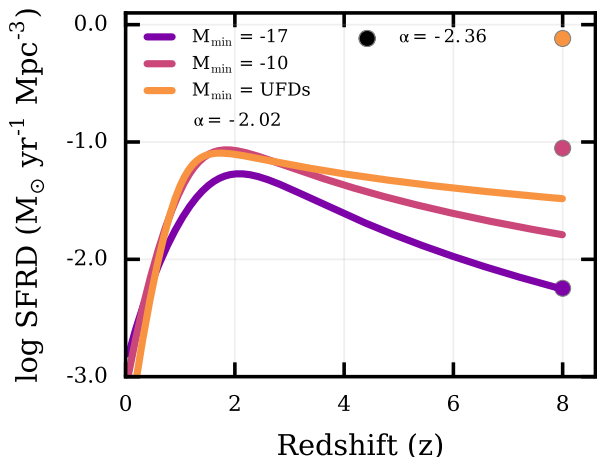


Figure 3. The cosmic SFH, with no correction for dust, computed by integrating literature UVLFs at each redshift to different values of M_{\min} and assuming $\alpha = -2.02$ at $z \sim 8$. The solid purple line is the fiducial cosmic SFH from [Madau & Dickinson \(2014\)](#). The magenta line reflects the cosmic SFH when $M_{\min} = -10$, the canonical faint limit for galaxies to maintain reionization (e.g., [Robertson et al. 2015](#)), while the orange line includes the contribution of UFDs. The solid points at $z \sim 8$ illustrate the effects of the steeper faint-end slope ($\alpha = -2.36$) as reported in [Finkelstein et al. \(2015\)](#). Including UFDs in the calculation of the cosmic SFH can boost the SFR density of the Universe by factors of $\gtrsim 4 - 100$ at $z \gtrsim 6$ if the UVLF remains steep.

there are still too many uncertainties that could mitigate this concern. For example, the stellar fossil record of UFDs is not yet capable of differentiating between star formation that started at $z \sim 10$ and $z \sim 12$ (100 Myr in time), which is required to directly compare measurements from UFDs with constraints from Planck. For this paper, we have adopted $z \sim 11$ for the start of star formation. This is in some tension ($< 2\sigma$) with Planck constraints on τ_e , but only if the UVLF is very steep at $z \gtrsim 10$.

3.1.2 Cosmic Star Formation History

The cosmic SFH is typically derived by adopting a fixed (and fairly bright) lower bound for integration of the UVLFs at all redshifts (such as $L=0.03 L_{\star}$ or $M_{\min} \sim -17$; e.g., [Madau et al. 2014](#)). Very faint, star-forming galaxies in the early Universe have a substantial effect on the cosmic star formation rate (SFR) density at $z \sim 6 - 8$ in the steep faint-end slope scenario.

Figure 3 shows that adopting fainter limits substantially affects the cosmic SFH for $z \gtrsim 6$. In this Figure, we have fit the functional form of the cosmic SFH from Equation 15 in [Madau et al. \(2014\)](#) to several of the same UVLFs from the literature used by [Madau et al. \(2014\)](#), adopting the same UV-to-SFR conversion factor (and making no corrections for extinction). The various colored lines in Figure 3 show the cosmic SFH integrated to three values of M_{\min} : -17 (solid purple), -10 (solid magenta), and values shown in Figure 1 for $z \gtrsim 3$ and -10 otherwise (solid orange). The colored points at $z \sim 8$ indicate changes to the cosmic SFH if the steeper faint-end slope of $\alpha = -2.36$ is used ([Finkelstein et al. 2015](#)).

Relative to the fiducial assumptions (solid purple), adopting $M_{\min} = -10$ increases the SFR density of the Universe by a factor of $\sim 2-3$ for $z \gtrsim 6$. Adopting values of M_{\min} from the faintest UFDs yields an increase by factors of $\sim 4-6$. At $z \sim 8$, selecting the steeper faint-end slope ($\alpha = -2.36$) results in substantial changes in the cosmic SFH: an increase by a factor of ~ 15 for $M_{\min} = -10$ (magenta point) and ~ 130 for $M_{\min} = -3.1$ (orange point). Such large increases are also expected at $z \sim 9 - 10$ if the faint-end slope is steep ($\alpha = -2.3$; e.g., [Bouwens et al. 2016](#)). The large (100x) increase in SFRs implied by the very steep faint-end slopes at $z \gtrsim 6$ may be odds with the SFR density implied by high-redshift gamma-ray burst observations (e.g., [Kistler et al. 2009, 2013](#); [Chary et al. 2016](#)). However, it remains unclear if current GRB measurements are unbiased tracers (e.g., that they trace UFDs) of the total SFR density of the Universe (e.g., [Madau & Dickinson 2014](#)).

3.1.3 Dark Matter Halo Masses

Establishing the halo masses of faint galaxies in the early Universe is central to our understanding of primordial galaxy formation. Using the stellar-halo mass relation (SMH) as described in [Boylan-Kolchin et al. \(2014\)](#), we estimate that a galaxy with $M_{UV}(z = 7) = -3.1$ is hosted in a halo with $M_{\text{halo}}(z = 7) \sim 10^6 M_{\odot}$. This result is not very sensitive to the adopted SMH relation.

Taken at face value, this halo mass seems in reasonable agreement with predictions for the first mini-halos (e.g., [Wise et al. 2012](#)). However, it is also well-below the virial mass ($\sim 10^8 M_{\odot}$) that corresponds to the atomic cooling limit (10^4 K) at $z \sim 7$. Galaxy formation in such low-mass halos is expected to be very inefficient, owing to a strong reliance on molecular cooling. If the UVLF remains steep into the regime of UFDs, then there should be a substantial population of UFDs observable in the Local Group (e.g., [Boylan-Kolchin et al. 2014, 2015](#)). However, $\lesssim 10\%$ of the predicted number of extremely low-mass galaxies are known to exist in the LG (e.g., see updates to [McConnachie 2012](#)).

While environmental effects (e.g., efficient destruction of satellites, dwarf-dwarf mergers, stellar stripping) could alleviate some tension, these mechanisms do not appear efficient enough to resolve the discrepancy (e.g., [Kirby et al. 2013](#); [Deason et al. 2014](#); [Garrison-Kimmel et al. 2017](#)). Further, the over-abundance of LG dwarfs is not limited to the faintest UFDs, as it is known to persist in the ‘classical’ dwarf regime ([Boylan-Kolchin et al. 2015](#)), which is thought to be observationally complete (e.g., [Koposov et al. 2008](#)).

Even more challenges arise if (a) the faint-end of the UVLF approaches $\alpha = -2.4$ (i.e., many more faint galaxies) and/or (b) such low-mass galaxies have a low star-formation duty cycle (e.g., $\sim 10\%$; [Wyithe et al. 2014](#)). In the latter case, 90% of the halos would be in the ‘off’ state at any given time, and thus have reduced UV luminosities. Effectively, this results in higher-luminosity galaxies hosted in even lower-mass halos, assuming a canonical abundance matching relationship.

3.2 Minimizing the Flux Contribution of Ultra-Faint Dwarfs

Up to this point, we have considered the consequences of extrapolating a Schechter UVLF into the regime of UFDs. However, several numerical simulations of galaxy formation predict a turnover in the UVLF, decreasing the predicted number of very faint galaxies in the early Universe (e.g., Jaacks et al. 2013; O’Shea et al. 2015; Gnedin 2016; Liu et al. 2016; Ocvirk et al. 2016; Yue et al. 2016; Finlator et al. 2017). Although details vary, the common threads among these simulations are that not all low-mass halos necessarily host a galaxy and that baryonic effects internal to the galaxies (e.g., supernovae feedback, radiation pressure) can significantly affect galaxy formation in low-mass halos. Alternately, a turnover in the high- z UVLF is consistent with models that suppress or eliminate small-scale structure (e.g., Warm Dark Matter; Schultz et al. 2014; Dayal et al. 2015). A broken LF at high- z is also necessary in order to avoid dramatically overproducing UFDs and even classical dwarfs in the Local Group (Boylan-Kolchin et al. 2014, 2015).

Figure 4 illustrates the effects of two plausible UVLF turnovers. For simplicity, we focus only the $z = 7$ case and adopt analytic UVLFs that turnover from Jaacks et al. (2013) and Boylan-Kolchin et al. (2015). The Boylan-Kolchin et al. (2015) UVLF has $\alpha \sim -2$ for $M_{UV} < -13$ and $\alpha \sim -1.2$ for $M_{UV} \geq -13$ and is designed to reproduce $z = 0$ LG dwarf galaxy counts. For illustrative purposes, we have tuned the UVLF from Equation 1 in Jaacks et al. (2013) to match the general shape of Boylan-Kolchin et al. (2015).

The bottom panel of Figure 4 shows the cumulative fraction of UV flux for the UVLFs in the top panel. The decreased number density for UFDs reduces their UV flux contribution to $\lesssim 10\%$. We emphasize that this figure only provides an illustration of the effects of a turnover in the UVLF and it not necessarily correct in detail. Further, there is already tentative evidence that the UVLF remains steep at $z \sim 6$ down to at least $M_{UV} \sim -12.5$ (Livermore et al. 2016), which would be in tension with our selected turnover parameters (though see Bouwens et al. 2016).

Beyond matching local galaxy counts and reducing the contribution of UFDs to reionization, any turnover in the UVLF also affects the SHM relation. The UVLFs with a turnover in Figure 4 place $M_{UV}(z = 7) = -3.1$ UFDs in halos with $M_{\text{halo}}(z = 7) = 2 \times 10^8 M_{\odot}$ instead of $\sim 10^6 M_{\odot}$. Such a turnover therefore places the faintest galaxies in halos above the atomic cooling limit, resolving another possible tension implied by a steep UVLF.

4 SUMMARY

By combining the stellar fossil record of known UFDs in the Local Group with population synthesis modeling, we have demonstrated that star-forming galaxies with UV luminosities as faint as $M_{UV} = -3$ to -6 existed during the epoch of reionization ($z \sim 6 - 10$) must have existed. We explored the implications of this result under two possible scenarios, which can be summarized as follows:

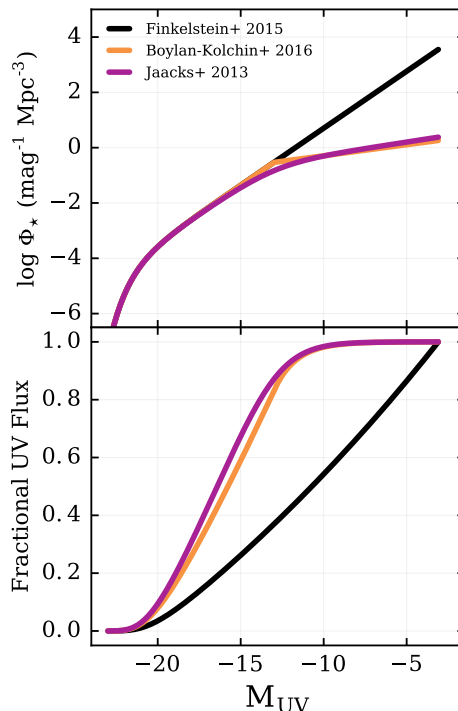


Figure 4. *Top* – A comparison between the UVLFs at $z \sim 7$ with and without turnovers. The steep UVLF (black; $\alpha \sim -2$) is from Finkelstein et al. (2015), while the other curves show models from Boylan-Kolchin et al. (2015, orange) and Jaacks et al. (2013, magenta). *Bottom* – The fraction of UV flux at $z \sim 7$ for each of the UVLFs shown in the top panel, when integrated to $M_{\text{min}} = -3.1$. A break or turnover in the UVLF at $M_{UV} = -13$ significantly reduces the flux contribution from UFDs.

If the measured high-redshift UVLFs with steep faint-end slopes are valid into the luminosity regime of UFDs:

- Galaxies fainter than $M_{UV} = -10$ contribute $>50-80\%$ of the total UV flux from galaxies during reionization.
- Galaxies can still power reionization with escape fractions that are $>50\%$ lower than currently assumed.
- The ancestors of UFDs must have been hosted in halos with $M_{\text{halo}}(z \sim 7) \sim 10^6 M_{\odot}$, well below the virial mass that corresponds to the atomic cooling limit.
- There should be ~ 10 times more galaxies around the MW with luminosities as bright as Draco ($M_V = -8.8$).

If the high- z galaxy UVLF turns over at $M_{UV}(z = 7) \sim -13$:

- UFDs do not contribute substantially to reionization at $z \lesssim 8$.
- There is no number galaxy count tension in the LG.
- UFDs live in halos more massive than the virial mass associated with the atomic cooling limit.

A complete census of Local Group UFDs has the promise to provide a robust constraint on the faint end of high- z UVLFs. Even with the current census, a scenario in which the high- z luminosity function is sharply truncated at magnitudes significantly brighter than $M_{UV} \sim -3$ to -6 is inconsistent with the existence of UFDs in the Local Group.

Thus, it appears unavoidable that the galaxy luminosity function extends, without a sharp truncation, to luminosities that are $\sim 10,000\times$ fainter than the blank-field UDF limits.

ACKNOWLEDGEMENTS

The authors thank Ben Johnson for help with correctly translating SFHs to UV fluxes, and Peter Behroozi, James Bullock, Eliot Quataert, Brian Siana, and Evan Skillman for useful discussions, particularly regarding the cosmic SFH. We acknowledge the extremely valuable discussions at the Near-far workshop in Santa Rosa, CA. DRW also thanks the SOC of the Galaxy Evolution III conference in Sesto for the invitation, which led to many new insights. MBK acknowledges support from the National Science Foundation (grant AST-1517226) and from NASA through HST theory grants AR-12836, AR-13888, AR-13896, and AR-14282 awarded by the Space Telescope Science Institute (STScI), which is operated by the Association of Universities for Research in Astronomy (AURA), Inc., under NASA contract NAS5-26555. Analysis and plots presented in this paper used IPython and packages from NumPy, SciPy, and Matplotlib (Hunter 2007; Oliphant 2007; Pérez & Granger 2007; Astropy Collaboration et al. 2013).

REFERENCES

- Astropy Collaboration et al., 2013, *A&A*, **558**, A33
 Bechtol K., et al., 2015, *ApJ*, **807**, 50
 Belokurov V., et al., 2006, *ApJ*, **647**, L111
 Belokurov V., et al., 2010, *ApJ*, **712**, L103
 Bouwens R. J., et al., 2014, *ApJ*, **793**, 115
 Bouwens R. J., et al., 2015, *ApJ*, **803**, 34
 Bouwens R. J., et al., 2016, *ApJ*, **830**, 67
 Bovill M. S., Ricotti M., 2009, *ApJ*, **693**, 1859
 Boylan-Kolchin M., Bullock J. S., Garrison-Kimmel S., 2014, *MNRAS*, **443**, L44
 Boylan-Kolchin M., Weisz D. R., Johnson B. D., Bullock J. S., Conroy C., Fitts A., 2015, *MNRAS*, **453**, 1503
 Brown T. M., et al., 2014, *ApJ*, **796**, 91
 Chary R., Petitjean P., Robertson B., Trenti M., Vangioni E., 2016, preprint, ([arXiv:1609.00764](https://arxiv.org/abs/1609.00764))
 Conroy C., Gunn J. E., White M., 2009, *ApJ*, **699**, 486
 Conroy C., White M., Gunn J. E., 2010, *ApJ*, **708**, 58
 Dayal P., Mesinger A., Pacucci F., 2015, *ApJ*, **806**, 67
 Deason A., Wetzel A., Garrison-Kimmel S., 2014, *ApJ*, **794**, 115
 Domínguez A., Siana B., Brooks A. M., Christensen C. R., Bruzual G., Stark D. P., Alavi A., 2015, *MNRAS*, **451**, 839
 Finkelstein S. L., et al., 2015, *ApJ*, **810**, 71
 Finlator K., et al., 2017, *MNRAS*, **464**, 1633
 Frebel A., Norris J. E., 2015, *ARA&A*, **53**, 631
 Fumagalli M., da Silva R. L., Krumholz M. R., 2011, *ApJ*, **741**, L26
 Garrison-Kimmel S., et al., 2017, preprint, ([arXiv:1701.03792](https://arxiv.org/abs/1701.03792))
 Girardi L., et al., 2010, *ApJ*, **724**, 1030
 Gnedin N. Y., 2016, *ApJ*, **825**, L17
 Hunter J. D., 2007, Computing in Science and Engineering, 9
 Irwin M. J., et al., 2007, *ApJ*, **656**, L13
 Jaacks J., Thompson R., Nagamine K., 2013, *ApJ*, **766**, 94
 Kim D., Jerjen H., Mackey D., Da Costa G. S., Milone A. P., 2015, *ApJ*, **804**, L44
 Kirby E. N., Cohen J. G., Guhathakurta P., Cheng L., Bullock J. S., Gallazzi A., 2013, *ApJ*, **779**, 102
 Kistler M. D., Yüksel H., Beacom J. F., Hopkins A. M., Wyithe J. S. B., 2009, *ApJ*, **705**, L104
 Kistler M. D., Yüksel H., Hopkins A. M., 2013, preprint, ([arXiv:1305.1630](https://arxiv.org/abs/1305.1630))
 Kopysov S., et al., 2007, *ApJ*, **669**, 337
 Kopysov S., et al., 2008, *ApJ*, **686**, 279
 Kopysov S. E., Belokurov V., Torrealba G., Evans N. W., 2015, *ApJ*, **805**, 130
 Kroupa P., 2001, *MNRAS*, **322**, 231
 Kuhlen M., Krumholz M. R., Madau P., Smith B. D., Wise J., 2012, *ApJ*, **749**, 36
 Laevens B. P. M., et al., 2015a, *ApJ*, **802**, L18
 Laevens B. P. M., et al., 2015b, *ApJ*, **813**, 44
 Leitet E., Bergvall N., Hayes M., Linné S., Zackrisson E., 2013, *A&A*, **553**, A106
 Liu C., Mutch S. J., Angel P. W., Duffy A. R., Geil P. M., Poole G. B., Mesinger A., Wyithe J. S. B., 2016, *MNRAS*, **462**, 235
 Livermore R. C., Finkelstein S. L., Lotz J. M., 2016, preprint, ([arXiv:1604.06799](https://arxiv.org/abs/1604.06799))
 Ma X., Kasen D., Hopkins P. F., Faucher-Giguère C.-A., Quataert E., Kereš D., Murray N., 2015, *MNRAS*, **453**, 960
 Madau P., Dickinson M., 2014, *ARA&A*, **52**, 415
 Madau P., Haardt F., 2015, *ApJ*, **813**, L8
 Madau P., Weisz D. R., Conroy C., 2014, *ApJ*, **790**, L17
 Martin N. F., et al., 2015, *ApJ*, **804**, L5
 McConnachie A. W., 2012, *AJ*, **144**, 4
 McQuinn M., 2012, *MNRAS*, **426**, 1349
 Oñorbe J., Boylan-Kolchin M., Bullock J. S., Hopkins P. F., Kereš D., Faucher-Giguère C.-A., Quataert E., Murray N., 2015, *MNRAS*, **454**, 2092
 O’Shea B. W., Wise J. H., Xu H., Norman M. L., 2015, *ApJ*, **807**, L12
 Ocvirk P., et al., 2016, *MNRAS*, **463**, 1462
 Okamoto S., Arimoto N., Yamada Y., Onodera M., 2012, *ApJ*, **744**, 96
 Oliphant T. E., 2007, Computing in Science and Engineering, 9
 Pérez F., Granger B. E., 2007, Computing in Science and Engineering, 9
 Planck Collaboration et al., 2016, *A&A*, **594**, A13
 Ricotti M., Gnedin N. Y., 2005, *ApJ*, **629**, 259
 Robertson B. E., et al., 2013, *ApJ*, **768**, 71
 Robertson B. E., Ellis R. S., Furlanetto S. R., Dunlop J. S., 2015, *ApJ*, **802**, L19
 Schultz C., Oñorbe J., Abazajian K. N., Bullock J. S., 2014, *MNRAS*, **442**, 1597
 Siana B., et al., 2015, *ApJ*, **804**, 17
 Stanway E. R., Eldridge J. J., Becker G. D., 2016, *MNRAS*, **456**, 485
 Stark D. P., 2016, *ARA&A*, **54**, 761
 Tollerud E. J., Bullock J. S., Strigari L. E., Willman B., 2008, *ApJ*, **688**, 277
 Walsh S. M., Willman B., Jerjen H., 2009, *AJ*, **137**, 450
 Weisz D. R., et al., 2012, *ApJ*, **744**, 44
 Weisz D. R., Dolphin A. E., Skillman E. D., Holtzman J., Gilbert K. M., Dalcanton J. J., Williams B. F., 2014a, *ApJ*, **789**, 147
 Weisz D. R., Dolphin A. E., Skillman E. D., Holtzman J., Gilbert K. M., Dalcanton J. J., Williams B. F., 2014b, *ApJ*, **789**, 148
 Weisz D. R., Johnson B. D., Conroy C., 2014c, *ApJ*, **794**, L3
 Willman B., et al., 2005, *AJ*, **129**, 2692
 Wise J. H., Abel T., Turk M. J., Norman M. L., Smith B. D., 2012, *MNRAS*, **427**, 311
 Wyithe J. S. B., Loeb A., Oesch P. A., 2014, *MNRAS*, **439**, 1326
 Yue B., Ferrara A., Xu Y., 2016, *MNRAS*, **463**, 1968
 Zucker D. B., et al., 2006a, *ApJ*, **643**, L103
 Zucker D. B., et al., 2006b, *ApJ*, **650**, L41